

**PHOTOCATALYTIC DEGRADATION OF PHENOL IN A  
FLUIDIZED BED REACTOR USING TiO<sub>2</sub> PREPARED BY A  
HYDROTHERMAL METHOD IMMOBILIZED ON GRANULAR  
ACTIVATED CARBON**

by

**SIN JIN CHUNG**

**Thesis submitted in fulfillment of the  
requirements for the degree  
of Master of Science**

**MAY 2010**

## ACKNOWLEDGEMENTS

First of all, I would like to express sincere gratitude to my supervisor, Prof. Abdul Rahman Mohamed for his valuable ideas, advices, suggestions and guidance throughout my postgraduate studies.

Secondly, I would like to grab this opportunity to thank all lecturers, staffs and technicians in School of Chemical Engineering especially Prof. Abdul Latif Ahmad, Assoc. Prof. Bassim H. Hameed, Dr. Zainal Ahmad, Pn. Aniza, En. Roqib and En. Faiza for their help and support. I would also like to thank the technicians of School of Material and Mineral Resources Engineering and School of Biology for the help with sample analyses.

I wish to thank Universiti Sains Malaysia for providing me the USM fellowship and Ministry of Science, Technology and Innovation Malaysia under the Science Fund (No. 6013338) for funding my project.

Special thanks to all my beloved friends especially Lam Sze Mun and not forgetting Fauziah, Liu Wei Wen and Siva Kumar for their help, kindness and moral support towards me. Thank you my friends.

Finally, I thank my parents Sin Boon Hwa and Ang Cheong Sim, brother Sin Jin Ming and sisters Sin Min Chyi and Sin Yuh Miin for their encouragement, moral and financial supports in all the good and hard times.

## TABLE OF CONTENTS

	Page
<b>ACKNOWLEDGEMENTS</b>	ii
<b>TABLE OF CONTENTS</b>	iii
<b>LIST OF TABLES</b>	vii
<b>LIST OF FIGURES</b>	ix
<b>LIST OF PLATES</b>	xii
<b>LIST OF SYMBOLS</b>	xiii
<b>LIST OF ABBREVIATIONS</b>	xv
<b>ABSTRAK</b>	xvii
<b>ABSTRACT</b>	xix
<b>CHAPTER ONE : INTRODUCTION</b>	
1.1 Treatment of industrial effluents	1
1.2 Photocatalysis in wastewater treatment	2
1.3 Problem statement	4
1.4 Research objectives	6
1.5 Scope of study	7
1.6 Organization of the thesis	7
<b>CHAPTER TWO : LITERATURE REVIEW</b>	
2.1 Advanced oxidation processes	10
2.2 Heterogeneous photocatalysis	12
2.2.1 Titanium dioxide as photocatalyst	15
2.2.2 Titanium dioxide assisted photocatalysis	17
2.3 Nanosized titanium dioxide	20
2.4 Synthesis of immobilized photocatalyst	22
2.5 Hydrothermal method	23
2.6 Supports for immobilization	25

2.7	Photocatalytic reactor	29
2.8	Phenol	32
2.9	Photodegradation of phenol	34
2.10	Effects of operating parameters	35
	2.10.1 Effect of photocatalyst loading	35
	2.10.2 Effect of pH	37
	2.10.3 Effect of electron acceptors	39
	2.10.4 Effect of initial pollutant concentration	40
2.11	Design of experiment (DOE)	42
	2.9.1 Response surface methodology (RSM)	42
	2.9.2 Central composite design (CCD)	45
2.12	Reaction kinetics	47

### **CHAPTER THREE : EXPERIMENTAL**

3.1	Materials and chemicals	50
3.2	Equipments	51
	3.2.1 Stainless steel Teflon-lined autoclave	51
	3.2.2 Fluidized bed reactor	53
3.3	Photocatalyst preparation	56
	3.3.1 Synthesis of TiO <sub>2</sub> sol	56
	3.3.2. Immobilization of TiO <sub>2</sub> onto GAC	57
3.4	Characterization studies	58
	3.4.1 X-ray Diffraction (XRD)	58
	3.4.2 Transmission electron microscopy (TEM)	58
	3.4.3 Scanning electron microscopy (SEM)	58
	3.4.4 Energy dispersive x-ray spectroscopy (EDX)	59
	3.4.5 Surface area and porosity measurement	59
3.5	Photocatalytic performance evaluation	60
	3.5.1 Control experiments	61
	3.5.2 Effect of hydrothermal temperature	61
	3.5.3 Immobilized versus suspended photocatalyst	61
	3.5.4 Catalytic activity of recycled TiO <sub>2</sub> /GAC	62

3.5.5	Migration studies	62
3.6	Effects of operating parameters	62
3.6.1	Effect of TiO <sub>2</sub> loading	62
3.6.2	Effect of inorganic anions	63
3.6.3	Effect of pH	63
3.6.4	Effect of air flow rate	63
3.6.5	Effect of H <sub>2</sub> O <sub>2</sub>	63
3.6.6	Effect of initial phenol concentration	64
3.7	Sample analyses	64
3.7.1	High Performance liquid chromatograph (HPLC)	64
3.7.2	Total organic carbon (TOC)	64
3.8	Experimental design and optimization	65

## **CHAPTER FOUR : RESULTS AND DISCUSSION**

4.1	Characterization of TiO <sub>2</sub> /GAC	69
4.1.1	X- ray Diffraction (XRD)	69
4.1.2	Transmission electron microscopy (TEM)	72
4.1.3	Scanning electron microscopy (SEM)	76
4.1.4	Energy dispersive X-ray (EDX)	77
4.1.5	Surface area and porosity	79
4.2	Identification of influencing factors on the photocatalytic activity	81
4.3	Effect of hydrothermal temperature on the photocatalytic performance	84
4.4	Comparison between immobilized TiO <sub>2</sub> and suspended TiO <sub>2</sub>	88
4.4.1	Phenol degradation	88
4.4.2	Mineralization of phenol	91
4.5	Catalytic activity of recycled TiO <sub>2</sub> /GAC	93
4.6	Migration of phenol from GAC to TiO <sub>2</sub> under UV irradiation	96
4.7	Effect of operating parameters	98

4.7.1	Effect of TiO <sub>2</sub> loading	98
4.7.2	Effect of inorganic anions	101
4.7.3	Effect of pH	104
4.7.4	Effect of air flow rate	108
4.7.5	Effect of H <sub>2</sub> O <sub>2</sub>	111
4.7.6	Effect of initial phenol concentration	115
4.8	Optimization studies of phenol degradation	119
4.8.1	Analysis of response surface	123
4.8.2	Optimization study and verification	127
4.9	Kinetic study of phenol degradation	128
4.9.1	Determination of kinetic order and apparent rate constant	130
4.9.2	Initial reaction rates	133

## **CHAPTER FIVE : CONCLUSIONS AND RECOMMENDATIONS**

5.1	Conclusions	136
5.2	Recommendations	138

<b>REFERENCES</b>	140
-------------------	-----

## **APPENDIX**

Appendix A	Calibration curve	165
------------	-------------------	-----

<b>LIST OF PUBLICATIONS</b>	166
-----------------------------	-----

## LIST OF TABLES

		Page
Table 2.1	Oxidation Potential of Different Oxidants (Molinari <i>et al.</i> , 2004)	10
Table 2.2	Band gap energy and corresponding radiation wavelength required for the excitation of several semiconductors (Robert, 2007)	13
Table 2.3	List of aqueous organic pollutants degraded by heterogeneous photocatalysis	14
Table 2.4	Chemical and physical properties of phenol (Busca <i>et al.</i> , 2008)	33
Table 2.5	Concentration of phenol from different industrial wastewaters (Priya <i>et al.</i> , 2008)	33
Table 2.6	List of optimal photocatalyst concentration of different types of organic pollutants and reactor designs	36
Table 3.1	List of chemical and materials	50
Table 3.2	Specification of UV lamps	54
Table 3.3	Experimental range and levels of independent variables	66
Table 3.4	Experimental conditions for photocatalytic degradation of phenol based on 3 level factorial designs in RSM analysis	66
Table 4.1	Crystalline phase, average crystallite size and relative anatase crystallinity of TiO <sub>2</sub> /GAC prepared at different hydrothermal temperatures	71
Table 4.2	EDX analysis	79
Table 4.3	BET surface area and porosity parameters of GAC and TiO <sub>2</sub> /GAC prepared at different hydrothermal temperatures	80
Table 4.4	TOC removal for TiO <sub>2</sub> /GAC and suspended Degussa P-25 during phenol degradation	91
Table 4.5	Experimental matrix and results	120
Table 4.6	Model fitting analysis	121

Table 4.7	ANOVA results of the quadratic model for the response of phenol degradation	122
Table 4.8	Factors and their desired goal for optimizing phenol degradation	127
Table 4.9	Experimental solution given by the software	127
Table 4.10	Values of $k_{app}$ and $R^2$ under different initial phenol concentrations	132



## LIST OF FIGURES

	Page	
Figure 2.1	Crystal structure of anatase, rutile and brookite of TiO <sub>2</sub> (Coronado <i>et al.</i> , 2008)	15
Figure 2.2	Energy diagram for TiO <sub>2</sub> and relevant redox potentials (Mills and Hunte, 1997)	17
Figure 2.3	Schematic representation of the processes occurring in photocatalysis upon irradiation of TiO <sub>2</sub> (Koči <i>et al.</i> , 2008)	18
Figure 2.4	A possible mechanism of phenol degradation (Guo <i>et al.</i> , 2006)	35
Figure 2.5	Response surface plot as presented by the Design-Expert software (Version 6.0.6, Stat-Ease, Inc., USA)	44
Figure 2.6	The three types of central composite design (NIST, 2006)	46
Figure 3.1	Schematic diagram of stainless steel Teflon-lined autoclave. (1) Magnetic stirrer, (2) Teflon, (3) TiO <sub>2</sub> colloidal solution, (4) Stainless steel plate, (5) Magnetic bar, (6) Heater, (7) Insulator, (8) Stainless steel cap, (9) Nut, (10) Pressure gauge, (11) Thermocouple, (12) Pressure release valve and (13) Nut	52
Figure 3.2	Schematic diagram of fluidized bed reactor. (1) Air compressor, (2) Air filter, (3) Pressure gauge, (4) Rotameter, (5) UV lamp, (6) Quartz glass column and (7) Thermocouple	55
Figure 3.3	Flow chart of the preparation of the TiO <sub>2</sub> sol	56
Figure 3.4	Flow chart of TiO <sub>2</sub> immobilization	57
Figure 4.1	XRD patterns of GAC and TiO <sub>2</sub> /GAC prepared at different hydrothermal temperatures: (a) GAC, (b) TiO <sub>2</sub> /GAC (120°C), (c) TiO <sub>2</sub> /GAC (150°C), (d) TiO <sub>2</sub> /GAC (180°C) and (e) TiO <sub>2</sub> /GAC (200°C)	70
Figure 4.2	TEM images of TiO <sub>2</sub> /GAC prepared at different hydrothermal temperatures: (a) TiO <sub>2</sub> /GAC (120°C), (b) TiO <sub>2</sub> /GAC (150°C), (c) TiO <sub>2</sub> /GAC (180°C) and (d) TiO <sub>2</sub> /GAC (200°C)	73
Figure 4.3	Schematic diagram of the mechanism for the formation	75

of TiO<sub>2</sub> in the hydrothermal treatment (Lee *et al.*, 2001; Lu and Wen, 2008)

Figure 4.4	SEM images of TiO <sub>2</sub> /GAC prepared at different hydrothermal temperatures: (a) TiO <sub>2</sub> /GAC (120°C), (b) TiO <sub>2</sub> /GAC (150°C), (c) TiO <sub>2</sub> /GAC (180°C) and (d) TiO <sub>2</sub> /GAC (200°C)	77
Figure 4.5	EDX spectrum of GAC	78
Figure 4.6	EDX spectrum of TiO <sub>2</sub> /GAC (180°C)	78
Figure 4.7	Photocatalytic degradation of phenol under different conditions. Conditions: TiO <sub>2</sub> loading = 322.2 mg/L, air flow rate = 2 L/min and C <sub>p</sub> = 50 mg/L	82
Figure 4.8	Effect of hydrothermal temperature on the photocatalytic degradation of phenol. Conditions: TiO <sub>2</sub> loading = 322.2 mg/L, air flow rate = 2 L/min and C <sub>p</sub> = 50 mg/L	85
Figure 4.9	Photocatalytic degradation of phenol using prepared TiO <sub>2</sub> /GAC and suspended Degussa P-25. Conditions: TiO <sub>2</sub> loading = 322.2 mg/L, air flow rate = 2 L/min and C <sub>p</sub> = 50 mg/L	89
Figure 4.10	Schematic illustration of mineralization of phenol over (a) TiO <sub>2</sub> /GAC and (b) Degussa P-25 powder (Zhang <i>et al.</i> , 2005)	92
Figure 4.11	Effect of recycling use of TiO <sub>2</sub> /GAC. Conditions: TiO <sub>2</sub> loading = 322.2 mg/L, air flow rate = 2 L/min, C <sub>p</sub> = 50 mg/L and t = 150 min	94
Figure 4.12	Concentration of phenol extracted from TiO <sub>2</sub> /GAC after being exposed to phenol solution for different times in the absence and presence of UV light. Conditions: TiO <sub>2</sub> loading = 322.2 mg/L, air flow rate = 2 L/min and C <sub>p</sub> = 50 mg/L	96
Figure 4.13	Effect of TiO <sub>2</sub> loading on the photocatalytic degradation of phenol. Conditions: pH = 5.2, air flow rate = 2 L/min and C <sub>p</sub> = 50 mg/L	99
Figure 4.14	Effect of inorganic anions on the photocatalytic degradation of phenol. Conditions: TiO <sub>2</sub> loading = 322.2 mg/L, pH = 5.2, air flow rate = 2 L/min and C <sub>p</sub> = 50 mg/L	101

Figure 4.15	Effect of pH on the photocatalytic degradation of phenol. Conditions: TiO <sub>2</sub> loading = 322.2 mg/L, air flow rate = 2 L/min and C <sub>p</sub> = 50 mg/L	105
Figure 4.16	Effect of air flow rate on the photocatalytic degradation of phenol. Conditions: TiO <sub>2</sub> loading = 322.2 mg/L, pH = 5.2 and C <sub>p</sub> = 50 mg/L	108
Figure 4.17	Effect of H <sub>2</sub> O <sub>2</sub> on the photocatalytic degradation of phenol. Conditions: TiO <sub>2</sub> loading = 322.2 mg/L, pH = 5.2, air flow rate = 2 L/min and C <sub>p</sub> = 50 mg/L	112
Figure 4.18	Effect of initial phenol concentration on the photocatalytic degradation of phenol. Conditions: TiO <sub>2</sub> loading = 322.2 mg/L, pH = 5.2 and air flow rate = 2 L/min	116
Figure 4.19	Predicted versus experimental values for phenol degradation percentage	123
Figure 4.20	Response surface plot for the effect of initial phenol concentration and TiO <sub>2</sub> loading on phenol degradation	124
Figure 4.21	Response surface plot for the effect of initial phenol concentration and H <sub>2</sub> O <sub>2</sub> concentration on phenol degradation	125
Figure 4.22	Response surface plot for the effect of TiO <sub>2</sub> loading and H <sub>2</sub> O <sub>2</sub> concentration on phenol degradation	126
Figure 4.23	Plot of ln C <sub>po</sub> /C <sub>p</sub> versus time for phenol degradation under different initial phenol concentrations. Conditions: TiO <sub>2</sub> loading = 322.2 mg/L, pH = 5.2 and air flow rate = 2 L/min	131
Figure 4.24	Linearization of the Langmuir-Hinshelwood model	134
Figure A-1	Calibration curve of phenol obtained from HPLC analysis	165

## LIST OF PLATES

	Page
Plate 3.1    Stainless steel Teflon-lined autoclave	52
Plate 3.2    Fluidized bed reactor	54
Plate 3.3    UV lamp enclosure with the quartz glass column	55

## LIST OF SYMBOLS

<b>Symbol</b>	<b>Description</b>	<b>Unit</b>
$C_p$	Phenol concentration	mg/L
$C_{po}$	Initial phenol concentration	mg/L
$dC_p/dt$	Differential of $C_p$ polynomial with respect to $t$	mg/L.min
$e^-$	Electron	-
$h^+$	Hole	-
$k$	Reaction rate constant	mg/L.min
$K$	Adsorption equilibrium constant	L/mg
$k_{app}$	apparent rate constant	1/min
$O_2\cdot^-$	Superoxide radical anion	-
$OH^-$	Hydroxyl ion	-
$\cdot OH$	Hydroxyl radical	-
$HO_2\cdot$	Hydroperoxyl radical	-
pzc	Point of zero charge	-
$R^2$	Correlation coefficient	-
$r$	reaction rate of phenol degradation	mg/L.min
T	Temperature	°C
$t$	Time	min
V	Volume of treated phenol solution	L

### Greek Symbols

$\sigma$	Standard deviation	-
$\lambda$	Wavelength of the UV lamp	nm

9

Surface coverage

-

## LIST OF ABBREVIATIONS

ANOVA	Analysis of variances
AOPs	Advanced oxidation processes
BET	Brunauer-Emmett-Teller
cb	Conduction band
CCD	Center composite design
CO <sub>2</sub>	Carbon dioxide
CV	Coefficient of variation
CVD	Chemical vapor deposition
3D	Three dimensional
<i>DF</i>	Degree of freedom
DOE	Department of Environment
EDX	Energy Dispersive X-ray spectroscopy
<i>F</i> value	Fisher value
FBR	Fluidized bed reactor
GAC	Granular activated carbon
HCl	Hydrochloric acid
H <sub>2</sub> O	water
H <sub>2</sub> O <sub>2</sub>	Hydrogen peroxide
HPLC	High pressure liquid chromatograph
<i>i</i> -PrOH	Isopropanol
NaCl	Sodium chloride
Na <sub>2</sub> CO <sub>3</sub>	Sodium carbonate
NaHCO <sub>3</sub>	Sodium bicarbonate
NaOH	Sodium hydroxide

Na <sub>2</sub> SO <sub>4</sub>	Sodium sulfate
O <sub>2</sub>	Oxygen
<i>Prob&gt;F</i>	Probability value greater than Fisher value
RSM	Response surface methodology
SEM	Scanning electron microscopy
TEM	Transmission electron microscopy
TiO <sub>2</sub>	Titanium dioxide
TiO <sub>2</sub> /GAC	Titanium dioxide immobilized on granular activated carbon
TTIP	Titanium (IV) isopropoxide
TOC	Total organic carbon
UV	Ultra-violet
vb	Valence band
XRD	X-Ray diffraction



# **DEGRADASI PEMFOTOMANGKINAN FENOL DI DALAM REAKTOR LAPISAN TERBENDALIR MENGGUNAKAN TiO<sub>2</sub> DARIPADA KAEDAH HIDROTERMA TERSEKAT GERAK PADA KARBON TERAKTIF**

## **ABSTRAK**

TiO<sub>2</sub> tersekat gerak pada karbon teraktif (TiO<sub>2</sub>/GAC) telah berjaya dihasilkan daripada kaedah hidroterma. Fotomangkin tersekat gerak yang disediakan dikaji dengan menggunakan XRD, TEM, SEM, EDX dan N<sub>2</sub> penyerapan. Aktiviti pemfotomangkinan bagi TiO<sub>2</sub>/GAC diselidik melalui degradasi fenol di dalam reaktor lapisan terbendalir. Keputusan menunjukkan bahawa fotomangkin tersekat gerak yang disediakan mempunyai hanya sejenis fasa kristal, iaitu anatis. Kekristalan dan saiz kristal bagi TiO<sub>2</sub>/GAC meningkat sepanjang suhu hidroterma dari 120°C ke 200°C. Morfologi permukaan fotomangkin tersekat gerak diselaputi oleh gumpalan TiO<sub>2</sub>. Keputusan EDX telah membuktikan kehadiran TiO<sub>2</sub> pada permukaan GAC. Luas permukaan dan jumlah kandungan lubang bagi TiO<sub>2</sub>/GAC didapati dipengaruhi oleh suhu hidroterma. Akan tetapi, purata kelebaran lubang ditunjukkan tidak banyak diubah. Efisiensi pemfotomangkinan bagi TiO<sub>2</sub>/GAC didapati dipengaruhi oleh suhu hidroterma dan optimum suhu hidroterma adalah 180°C. Kajian perbandingan keaktifan di antara TiO<sub>2</sub> tersekat gerak dan kormersial serbuk TiO<sub>2</sub> dijalankan pada keadaan eksperimen yang sama. TiO<sub>2</sub>/GAC didapati memberi keputusan yang lebih baik dalam degradasi fenol dan penghapusan jumlah karbon organik (TOC), iaitu 96.9% dan 85% masing-masing lebih tinggi daripada kormersial serbuk TiO<sub>2</sub>. Luas permukaan dan daya jerapan yang tinggi membolehkan GAC sebagai penyokong memainkan peranan yang baik dalam menjerap fenol, dan fenol yang terjerap dipindah dengan terus-menerus pada permukaan TiO<sub>2</sub>, di mana ia akan degradasi pemfotomangkinan. Selain itu, kecekapan pemfotomangkinan bagi TiO<sub>2</sub>/GAC adalah

menurun dengan sedikit selepas degradasi fenol selama empat kali. Keputusan untuk pembolehubah proses yang dikaji adalah: Bebanan  $\text{TiO}_2$  yang optimum adalah 322.2 mg/L; anion inorganik menunjukkan kesan negatif pada degradasi fenol dalam turutan  $\text{HCO}_3^- > \text{CO}_3^{2-} > \text{SO}_4^{2-} > \text{Cl}^-$ ; nilai pH yang optimum adalah 5.2; kadar aliran udara yang optimum adalah 2 L/min; degradasi fenol yang tinggi dapat dicapai dengan kepekatan  $\text{H}_2\text{O}_2$  pada 400 mg/L; degradasi fenol merosot bagi meningkatkan kepekatan awal fenol. Rekabentuk eksperimen berdasarkan metodologi permukaan sambutan (RSM) telah digunakan untuk menghasilkan degradasi fenol yang optimum. Maksima degrassi fenol pada 98.8 % dapat dicapai dengan kepekatan awal fenol pada 30 mg/L, bebanan  $\text{TiO}_2$  pada 2 lapisan (322.2 mg/L) dan kepekatan  $\text{H}_2\text{O}_2$  pada 200 mg/L. Akhirnya, kinetik degradasi fenol mematuhi model Langmuir-Hinshelwood. Nilai pemalar kadar dan nilai pemalar jerapan yang telah diperolehi adalah  $k = 8.18 \text{ mg/L.min}$  and  $K = 0.00086 \text{ L/mg}$  masing-masing.

**PHOTOCATALYTIC DEGRADATION OF PHENOL IN A FLUIDIZED BED REACTOR USING TiO<sub>2</sub> PREPARED BY A HYDROTHERMAL METHOD IMMOBILIZED ON GRANULAR ACTIVATED CARBON**

**ABSTRACT**

TiO<sub>2</sub> immobilized on granular activated carbon (TiO<sub>2</sub>/GAC) was successfully prepared using a hydrothermal method. The prepared photocatalysts were characterized by X-ray diffraction (XRD), transmission electron microscopy (TEM), scanning electron microscopy (SEM), energy dispersive X-ray (EDX) and N<sub>2</sub> physisorption. Their photocatalytic activities were evaluated through phenol degradation in a fluidized bed reactor. The characterization results revealed that the prepared photocatalysts had a single crystal phase, which was anatase. The crystallinity and crystal size of TiO<sub>2</sub>/GAC increased as the hydrothermal temperature increased from 120°C to 200°C. The surface morphology of prepared photocatalysts was agglomerated. EDX analysis confirmed the presence of TiO<sub>2</sub> on the surface of the GAC supports. The surface area and total pore volume of prepared photocatalysts were significantly affected by hydrothermal temperature. However, no much change was found on the average pore diameter. The photocatalytic efficiency of TiO<sub>2</sub>/GAC was strongly influenced by hydrothermal temperature and the optimum hydrothermal temperature was 180°C. For the comparison, the same photocatalysis experiment was performed using commercial Degussa P25. TiO<sub>2</sub>/GAC had shown better phenol degradation and total organic carbon removal (TOC), which was 96.9 % and 85 %, respectively higher than that of commercial Degussa P-25. The GAC support with high surface area and adsorption capacity had worked well for the phenol adsorption, and the adsorbed phenol migrated continuously onto the surface of TiO<sub>2</sub>, where it is photocatalytically degraded. Moreover, the photocatalytic ability of TiO<sub>2</sub>/GAC was

decreased slightly after four cycles for phenol degradation. The results for the studied operating parameters were: optimum TiO<sub>2</sub> loading was 322.2 mg/L; the inorganic anions had a negative effect on the phenol degradation in the order of HCO<sub>3</sub><sup>-</sup> > CO<sub>3</sub><sup>2-</sup> > SO<sub>4</sub><sup>2-</sup> > Cl; the optimum pH was found to be 5.2; the air flow rate gave an optimum value of 2 L/min; high phenol degradation can be achieved at H<sub>2</sub>O<sub>2</sub> concentration of 400 mg/L; the increase of initial phenol concentration gave a lower phenol degradation. An experimental design based on response surface methodology (RSM) was employed to optimize the phenol degradation. A maximum phenol degradation of 98.8 % was obtained at 30 mg/L of initial phenol concentration, 2 layers of TiO<sub>2</sub> loading (322.2 mg/L) and 200 mg/L of H<sub>2</sub>O<sub>2</sub> concentration. Finally, the kinetics of phenol degradation was fitted well with the Langmuir-Hinshelwood model. The reaction rate constant and the adsorption constant were calculated to be  $k = 8.18$  mg/L.min and  $K = 0.00086$  L/mg, respectively.

# CHAPTER ONE

## INTRODUCTION

### 1.1 TREATMENT OF INDUSTRIAL EFFLUENTS

Contamination of water by industrial effluents is a serious problem experienced by nations throughout the developed and developing world. Recently, rapid industrial expansion especially petrochemical, pharmaceutical, textile, agricultural, food and chemical industries all produce waste effluent contaminated with organic compounds such as aromatics, haloaromatics and dyes has contributed to the contamination of fresh water in the ecosystem (Robertson *et al.*, 2005). The released of untreated organic pollutants are of high priority concern since they are harmful to the environment and even their contamination in water at a few mg/L levels are highly carcinogenic to human and animals. In Malaysia, the number of water pollution sources was reported increase by 26 % from 13992 sources in 2000 to 18956 sources in 2006 (WHO, 2005; DOE, 2006). In this regard, a stricter water quality control standard and regulation such as Environmental Quality Act has been implemented in Malaysia in an effort to achieve a goal in environmental protection management policy. Therefore, the enforcement of the existing environmental laws is essential to ensure the capability of the industrial sector in destructing the potentially harmful compounds from the effluent before safe disposal into the natural waters.

A variety of conventional biological, chemical and physical methods are presently available to treat the harmful compounds in the effluents. However, these conventional wastewater treatments have limitations of their own in order to reach the degree of purity required for final use. Biological treatment (aerobic or anaerobic

digestion) usually is not effective in wastewater treatment due to some of the toxic compounds present in the industrial effluent are found not readily biodegradable and may kill the active microbes (Sanromán *et al.*, 2004). Chemical treatment (chlorination and ozonation) gave particular problems where chlorinated organic compounds as by-product after the chlorination treatment can be generated (Moonsiri *et al.*, 2004). Due to its instability and hazardous nature, the use of ozone may be more harmful to the environment (Bizani *et al.*, 2006). Finally, physical treatment (charcoal adsorption, reverse osmosis and ultrafiltration) is non-destructive and usually comprises a simple transfer of organic pollutants from a dispersed phase to a concentrated phase (Kabir *et al.*, 2006), thus causing secondary pollution.

In this way, new and more efficient treatment technologies to degrade the complex refractory molecules into simpler molecules must be considered to reduce the deteriorating water quality.

## **1.2 PHOTOCATALYSIS IN WASTEWATER TREATMENT**

In recent years, heterogeneous photocatalysis is one of the advanced oxidation processes (AOP) that has been accepted as a promising new alternative method in the area of wastewater treatment (Chen and Ray, 1999; Bekkouche *et al.*, 2004; Cao *et al.*, 2005; Liu *et al.*, 2007; Merabet *et al.*, 2009a). Compared with conventional wastewater treatments, heterogeneous photocatalysis has such advantages as: (1) pollutants are not merely transferred from one phase to another, but they are chemically transformed and completely mineralized to environmentally harmless compounds (2) this process is immune to organic toxicity to make it attractive for the degradation of toxic organic compounds and (3) this process has the

potential to utilize sunlight or visible light for irradiation, thereby advantageous to economic saving especially for large-scale operations (Chang *et al.*, 2005; Yu *et al.*, 2007a).

Generally, three basic components must be present in heterogeneous photocatalysis in order for the reaction to take place: an emitted photon (in the appropriate wavelength), a catalyst surface (usually TiO<sub>2</sub>) and oxygen (Lasa *et al.*, 2006). Photocatalytic process occurs when the catalyst is activated by UV light and followed by the excitation of an electron from the valence band to conduction band, leaving a positive hole behind in the valence band. These positively charged holes will react with water molecules leading to the formation of the hydroxyl radicals ( $\bullet\text{OH}$ ), which acts as strong oxidants to degrade the organic molecules (Zhang *et al.*, 2005a).

Two modes of TiO<sub>2</sub> as photocatalyst: (1) suspended TiO<sub>2</sub> powder and (2) immobilized TiO<sub>2</sub> are typically used in the photocatalytic degradation processes. Both types of TiO<sub>2</sub> offered various advantages and disadvantages. Suspended TiO<sub>2</sub> powder has been the most commonly used because of its simplicity and offers high surface area for reaction with almost no mass transfer limitation. Nevertheless, additional separation processes are required to recover the TiO<sub>2</sub> powder at the end of the treatment, either by filtration or centrifugation which is expensive in term of time and cost. Another concern is suspended TiO<sub>2</sub> powder tends to agglomerate into larger particles at high concentration, which reduces the catalytic activity. Thus, in terms of large scale application, immobilized TiO<sub>2</sub> is preferable. However, there is another problem that activity of immobilized TiO<sub>2</sub> system may be lower than the slurry

system due to reduction in surface area and mass transfer limitation (Li *et al.*, 2005; Damodar and Swaminathan, 2008; Song *et al.*, 2008).

### 1.3 PROBLEM STATEMENT

In recent years, increasing use of immobilized photocatalyst in the heterogeneous photocatalysis has witnessed its significant application in the wastewater treatment (Kang, 2002; Zhang *et al.*, 2006; Zhu and Zou, 2009). Even though immobilized TiO<sub>2</sub> allows the ease in continuous use of the photocatalyst by eliminating the need of additional separation processes in a slurry system, there are still technical challenges that must be further investigated and overcome. It is well established that the photocatalytic performance of TiO<sub>2</sub> are strongly influenced by the physiochemical properties such as crystallinity, crystal size and surface area, which are governed by the preparation method (Jang *et al.*, 2001; Senthilkumaar *et al.*, 2006; Tian *et al.*, 2009). Synthesis of immobilized nanosized TiO<sub>2</sub> is important to compensate the reduced performances associated with the immobilization process due to its large surface area and consistent with a high volume fraction of active sites available on the surface for substrate adsorption. Hence, knowledge especially in the synthesis of immobilized nanosized TiO<sub>2</sub> still requires better understanding.

As most commonly known, sol-gel, chemical vapour deposition (CVD) and hydrothermal are prominent methods for the synthesis of TiO<sub>2</sub>. Sol-gel and CVD usually generate a relatively homogeneous TiO<sub>2</sub> coating but require high calcination temperature above 450°C to induce crystallization. This is not economical and can cause crystal growth (Shang *et al.*, 2003; Sayilkan *et al.*, 2007). To avoid these defects, hydrothermal has been considered as an alternative method for the



preparation of immobilized TiO<sub>2</sub> in a nanocrystalline state, where low reaction temperature is employed, and physiochemical properties such as crystal size, morphology and crystalline phase of the prepared photocatalyst can be controlled (Kolen'ko *et al.*, 2003; Yu *et al.*, 2005; Zhao *et al.*, 2007).

Besides, the selection of a proper substrate as support for immobilized TiO<sub>2</sub> is essential to increase the photocatalytic degradation activities. Early works mainly focused on coating TiO<sub>2</sub> on non-adsorbent supports such as glass, quartz sand and stainless steel substrate (Shang *et al.*, 2003; Sonawane *et al.*, 2004; Pozzo *et al.*, 2006). The photocatalyst separation problem can somewhat be solved, but no improvement in the photoefficiency is observed due to the diffusion limitation of pollutants to the surface of TiO<sub>2</sub>. To avoid this problem, much attention is given to support TiO<sub>2</sub> on adsorptive materials such as zeolite, activated carbon (AC) and silica gel (Zhang *et al.*, 2006; Mahalakshmi *et al.*, 2009; Sun *et al.*, 2009). Among these supports, AC is used in this study owing to its superiority of adsorption capacity, high surface area and lower cost (Sun *et al.*, 2009)

In addition, an effective reactor design is considered important in the photocatalytic degradation reaction where intimate contact can be achieved between UV light, photocatalyst and reactants. In this sense, fluidized bed reactor is believed can increase the photocatalytic efficiency owing to its excellent reactant contact, high photocatalyst loading and efficient UV light exposure (Nam *et al.*, 2002; Nelson *et al.*, 2007). However, technical development of fluidized bed reactor is still not widely studied in heterogeneous photocatalysis technology for wastewater treatment. Thus, it is imperative to conduct a thorough study on the effect of operating

parameters to investigate the photocatalytic performance of the prepared photocatalyst in a fluidized bed reactor. The importance of the present work is to exploit the wide and ever-growing application of TiO<sub>2</sub> photocatalysis to be more practical in the wastewater treatment by studying the criteria in synthesis of immobilized TiO<sub>2</sub> with its photocatalytic performance in a fluidized bed reactor.

#### **1.4 RESEARCH OBJECTIVES**

The aim of this research is to develop an immobilized photocatalyst with high photoactivity, which is capable of degrading and mineralizing phenol under UV irradiation. The objectives of this research include:

1. To synthesize nanosized TiO<sub>2</sub> immobilized on granular activated carbon (TiO<sub>2</sub>/GAC) using a hydrothermal method.
2. To characterize the prepared TiO<sub>2</sub>/GAC based on its chemical and physical properties.
3. To study the performance of TiO<sub>2</sub>/GAC and effects of operating parameters such as TiO<sub>2</sub> loading, inorganic anions, pH, air flow rate, H<sub>2</sub>O<sub>2</sub> concentration and initial phenol concentration on photocatalytic degradation of phenol in a fluidized bed reactor.
4. To obtain optimum operating parameters by using response surface methodology.
5. To study the kinetic of photocatalytic degradation of phenol over TiO<sub>2</sub>/GAC.

## **1.5 SCOPE OF STUDY**

This research is focused on the development of highly effective immobilized TiO<sub>2</sub> prepared using hydrothermal method. The development of the photocatalyst includes studying the effect of hydrothermal temperature (120°C – 200°C) and GAC as support, on the TiO<sub>2</sub> photocatalytic activity. The freshly prepared immobilized photocatalyst are characterized using X-ray diffraction (XRD), transmission electron microscopy (TEM), scanning electron microscope (SEM), energy dispersive X-ray spectroscopy (EDX) and N<sub>2</sub> physisorption. Their photocatalytic activities are evaluated through phenol degradation in a fluidized bed reactor.

Various operating parameters such as TiO<sub>2</sub> loading (1 layer – 4 layers), pH (3.0 – 11.0), inorganic anions (Cl<sup>-</sup>, HCO<sub>3</sub><sup>-</sup>, CO<sub>3</sub><sup>2-</sup> and SO<sub>4</sub><sup>2-</sup>), air flow rate (1.0 L/min – 3.0 L/min), H<sub>2</sub>O<sub>2</sub> concentration (50 mg/L – 400 mg/L) and initial phenol concentration (20 mg/L – 110 mg/L) are studied to evaluate the photocatalytic performance of TiO<sub>2</sub>/GAC in a fluidized bed reactor. Data analysis is further studied using 2<sup>3</sup> factorial experimental design of response surface methodology (RSM) to optimize and analyze the possible interaction between the process variables on phenol degradation. Finally, kinetic study based on Langmuir-Hinshelwood kinetics model is studied to determine the rate of reaction in the phenol degradation.

## **1.6 ORGANIZATION OF THESIS**

There are five chapters in this thesis. Chapter 1 (Introduction) provides a brief description of treatment of industrial effluent and photocatalysis in wastewater treatment. This chapter also includes the problem statement that describes the problem faced and the needs of the current research. The objectives and scopes of

this study are then explained in this chapter. This is followed by the organization of the thesis.

Chapter 2 (Literature Review) provides the past research works in the photocatalysis field. A brief explanation about advanced oxidation process is in the first part and followed by the overview of photocatalysis. Subsequently, information regarding with the  $\text{TiO}_2$  as a photocatalyst, the immobilization onto the support and photocatalytic reactor are discussed in the second part. Next, the characteristic of phenol and details of phenol degradation are described. The effects of various operating parameters that affect the photocatalytic activity are included. Finally, the design of experiment (DOE) is discussed.

Chapter 3 (Materials and Methods) covers the experimental part. Details of the materials and chemical reagents with a general description about the photocatalytic reactor that are used in the present study are described in the first part. This is followed by the discussion on the detailed photocatalyst preparation and characterization techniques throughout this research. Lastly, process studies and experimental design are described in this chapter.

Chapter 4 (Results and Discussion) presents the experimental findings together with discussion. It is divided into eight parts: (a) characterization of  $\text{TiO}_2/\text{GAC}$ , (b) Effect of hydrothermal temperature on the photocatalytic performance, (c) determination of factors affecting the photocatalytic activity, (d) performance comparison between immobilized  $\text{TiO}_2$  and suspended  $\text{TiO}_2$ , (e)

extraction studies, (f) effect of operating parameters, (g) optimization studies and (h) kinetics studies.

Chapter 5 (Conclusions and Recommendations) summarizes the results reported in chapter 4 and recommends the possible ways to improve the present studies for future research in this field.

## CHAPTER TWO

### LITERATURE REVIEW

#### 2.1 ADVANCED OXIDATION PROCESSES

Since the early 1990s, a lot of research works have been carried out on special class of oxidation technique that is defined as advanced oxidation processes (AOPs) in wastewater treatment (Mills and Hoffmann, 1993; Minero *et al.*, 1995; Andreozzi *et al.*, 1999; Fernando *et al.*, 2003; Popiel *et al.*, 2009). It had shown that AOPs are a promising wastewater treatment technology could successfully work best for the near ambient degradation or mineralization of soluble organic pollutants from water and volatile organic compounds (VOCs) from air as well.

All AOPs are mainly based on hydroxyl radical ( $\bullet\text{OH}$ ) chemistry.  $\bullet\text{OH}$  radicals are powerful oxidizing agent responsible to oxidize the organic pollutants and have the second highest oxidizing potential. In Table 2.1, the oxidation potentials of some important oxidizing agents are listed.

Table 2.1: Oxidation Potential of Different Oxidants (Molinari *et al.*, 2004).

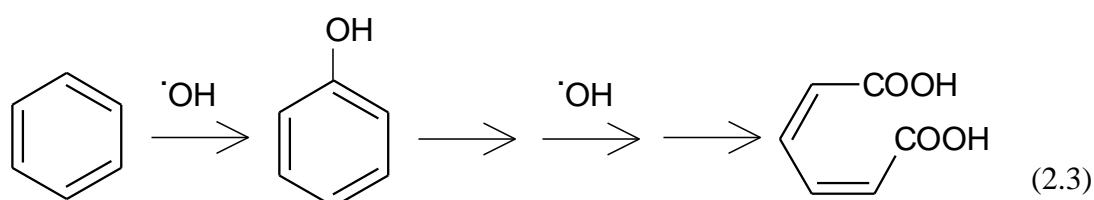
Oxidant	Oxidation Potential (eV)
Fluorine	3.03
<b>Hydroxyl radical</b>	<b>2.80</b>
Atomic oxygen	2.42
Ozone	2.07
Hydrogen peroxide	1.78
Perhydroxyl radical	1.70
Permanganate	1.68
Chlorine dioxide	1.57
Chlorine	1.36

From Table 2.1,  $\bullet\text{OH}$  radicals is the best choice for use in oxidation processes since it can be generated *in situ*, and compared to fluorine, oxidation products of  $\bullet\text{OH}$

radicals are less toxic with the possibility of complete mineralization of the organic pollutants (Ray *et al.*, 2006). Once the  $\bullet\text{OH}$  radicals generated, they can strongly react with most organic pollutants (RH) by hydrogen abstraction to produce organic radical ( $\bullet\text{R}$ ). Subsequently, the produced organic radicals can further react with molecular oxygen to give peroxy radicals, initiating a sequence of oxidative degradation reactions which may lead to complete mineralization of the organic pollutants (Chiron *et al.*, 2000):



In addition,  $\bullet\text{OH}$  radicals may also attack the aromatic organic pollutants by ring hydroxylation. However, a further  $\bullet\text{OH}$  radicals attack would lead to the opening of the ring and the formation of open conjugated structure (Litter *et al.*, 2005):



Common AOPs that have been studied in the wastewater treatment include (a) chemical oxidation using hydrogen peroxide, ozone, hydrogen peroxide/ozone and Fenton's agents, (b) radiation methods such as UV irradiation, (c) combination of any one of (a) with any of (b), (d) heterogeneous photocatalysis using UV with semiconductor photocatalysis (Ray *et al.*, 2006). However, in this study, only heterogeneous photocatalysis will be focussed.

## 2.2 HETEROGENEOUS PHOTOCATALYSIS

Among AOPs, heterogeneous photocatalysis has recently gained importance in the area of wastewater treatment (Daneshvar *et al.*, 2003; Singh *et al.*, 2007; Wu *et al.*, 2009). The process is recognized as a promising new destructive technology that can lead to the total mineralization of most of the organic pollutants. Compared to other competing processes, heterogeneous photocatalysis has several advantages: (1) complete mineralization, (2) no waste disposal problem, (3) the reaction is inexpensive and (4) only mild temperature and pressure conditions are necessary (Chang *et al.*, 2000; Chang *et al.*, 2005).

In the heterogeneous photocatalysis, three components must be present in order for the reaction to take place: (1) an emitted photon (in the appropriate wavelength), (2) a semiconductor photocatalyst and (3) oxygen (Lasa *et al.*, 2006). The overall process can be divided into five independent steps: (1) diffusion of reactants to the surface of catalyst, (2) adsorption of reactants onto the surface, (3) reaction on the adsorbed phase, (4) desorption of products off the surface, and (5) removal of the product from the interfacial region (Pirkanniemi and Sillanpää 2002).

During the photocatalytic process, it usually starts with an illumination of a semiconductor photocatalyst with light of an appropriate wavelength. When a photon with an energy equal to or greater than the band gap energy ( $E_{bg}$ ) of the photocatalyst reaches to the photocatalyst surface, a conduction band electron ( $e_{cb}^-$ ) and valence band hole ( $h_{vb}^+$ ) are generated (Hu *et al.*, 2003; Silva *et al.*, 2006).  $E_{bg}$  is defined as the difference between the filled valence band and the empty conduction band of the photocatalyst, in the order of a few electron volts (Lasa *et al.*, 2006). The band gap



energy and the corresponding radiation wavelength required for the excitation of various semiconductors are shown in Table 2.2.

Table 2.2: Band gap energy and corresponding radiation wavelength required for the excitation of several semiconductors (Robert, 2007).

<b>Semiconductor</b>	<b>Band gap energy (eV)</b>	<b>Wavelength (nm)</b>
SnO <sub>2</sub>	3.9	318
TiO <sub>2</sub> (rutile)	3.0	413
TiO <sub>2</sub> (anatase)	3.2	388
ZnO	3.2	388
WO <sub>3</sub>	2.8	443
Cds	2.5	516
Fe <sub>2</sub> O <sub>3</sub>	2.3	539
GaAs	1.7	886
GaP	1.4	539

If charge separation is maintained, both charge carriers are migrated to the photocatalyst surface where they participate in redox reactions. Generally,  $h_{vb}^+$  is reacted with surface-bound H<sub>2</sub>O or OH<sup>-</sup>, which is electron donor to produce •OH radicals while  $e_{cb}^-$  is picked up by electron acceptor such as oxygen to generate superoxide radical anions (O<sub>2</sub>•<sup>-</sup>) (Tariq *et al.*, 2005). Both radicals are very reactive and strongly oxidizing, which capable of mineralizing most of the organic pollutants. The mechanism for the generation of the radicals is shown in Equation 2.4 to 2.6 (Shon *et al.*, 2005; Tariq *et al.*, 2005):



As the result, the carbon-containing pollutants are oxidized to carbon dioxide while the other elements bonded to the organic compounds are converted to anions such as nitrate, sulphate or chloride (Mukherjee and Ray, 1999). The list of organic pollutants that can be degraded by heterogeneous photocatalysis is shown in Table 2.3.

Table 2.3: List of aqueous organic pollutants degraded by heterogeneous photocatalysis.

<b>Class of organics</b>	<b>Examples</b>	<b>References</b>
Haloalkanes/haloalkenes	Chloroform, trichloroethylene, trichloromethane, tribromomethane, CCl <sub>4</sub>	Choi and Hoffman (1997); Cheung <i>et al.</i> (1998); Lee <i>et al.</i> (2001); Keshmiri <i>et al.</i> (2004)
Aliphatic alcohols	Methanol, ethanol	Piera <i>et al.</i> (2002); Nelson <i>et al.</i> (2007)
Aliphatic carboxylic acids	Formic, citric	Kim and Anderson (1996); Quici <i>et al.</i> (2007)
Aromatics	Toulene	Martra <i>et al.</i> (1999)
Haloaromatics	2-chlorobiphenyl	Wang and Hong (2000)
Phenolic compounds	Phenol, catechol	Matos <i>et al.</i> (1998); Li <i>et al.</i> (2003); Tryba <i>et al.</i> (2008)
Halophenols	2,3-dichlorophenol, 4-chlorophenol, fluorophenol	4- Alhakimi <i>et al.</i> (2003) 4- Selvam <i>et al.</i> (2007); Liang <i>et al.</i> (2008)
Aromatic carboxylic acids	Malic, chlorobenzoic acids,	Han <i>et al.</i> (2004); Danion <i>et al.</i> (2007)
Surfactants	Sodium lauryl sulfate,	Nam <i>et al.</i> (2009)
Herbicides	Atrazine, alachlor	Wong and Chu (2003); Parra <i>et al.</i> (2004); Jain <i>et al.</i> (2009)
Pesticides/fungicides	monocrotophos, metalaxyl	Topalov <i>et al.</i> (1999); Shankar <i>et al.</i> , 2004
Dyes	Congo red, methyl orange, C.I. Reactive Red 198, indole, orange G	Nam <i>et al.</i> (2002); Sun <i>et al.</i> (2006); Wu (2008); Merabet <i>et al.</i> (2009b); Sun <i>et al.</i> (2009)

### 2.2.1 Titanium dioxide as photocatalyst

Although many semiconductors such as CdS, ZnO, Fe<sub>2</sub>O<sub>3</sub> and WO<sub>3</sub> have been employed as the photocatalyst for environmental remediation, titanium dioxide (TiO<sub>2</sub>) seems to be the most widely used photocatalyst because of its: (1) chemical stability, (2) robustness against photocorrosion, (3) low toxicity and (4) availability at low cost (Li *et al.*, 2005; Wang *et al.*, 2006).

TiO<sub>2</sub> is also known as titanium (IV) oxide or titania. The structure formula of the TiO<sub>2</sub> is O=Ti=O and its molecular mass is 79.87 g/mol. Melting point of the TiO<sub>2</sub> is 1870 °C while its boiling point is 2972 °C (Wikipedia). Besides, TiO<sub>2</sub> has three crystalline forms which are the anatase, rutile and brookite. Anatase and rutile are widely used in industrial applications, while the used of brookite is still rare due to its limited application (Thiruvengkatachari *et al.*, 2008). Crystal structures of anatase, rutile and brookite of TiO<sub>2</sub> are shown in Figure 2.1.

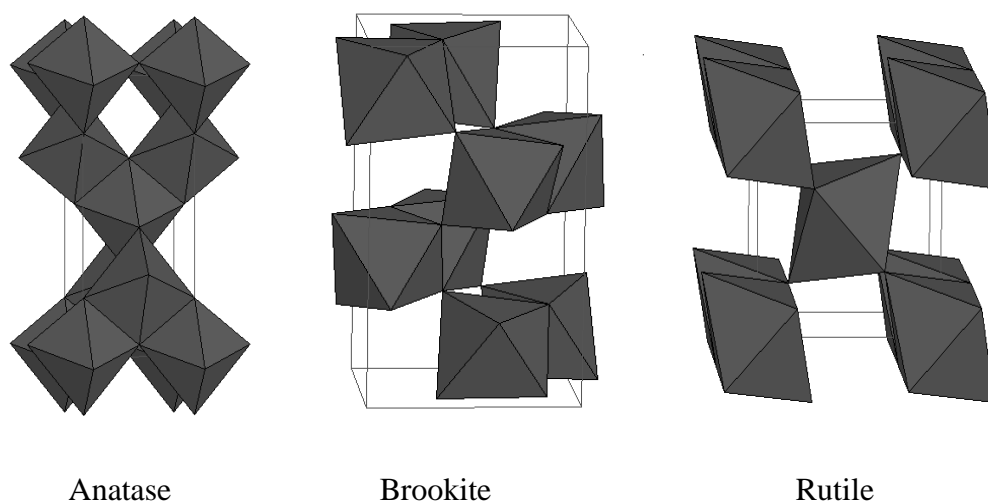


Figure 2.1: Crystal structure of anatase, rutile and brookite of TiO<sub>2</sub> (Coronado *et al.*, 2008).

From Table 2.2, rutile type of TiO<sub>2</sub> can absorb light of a wider range, which is slightly closer to visible light irradiation, it seem logical to assume rutile type is more suitable to be used as photocatalyst. Nevertheless, in reality, anatase type of TiO<sub>2</sub> is reported to exhibit a higher photocatalytic activity (Silva and Faria, 2009). One of the reasons is because the formation of anatase is favoured at lower temperature (< 600°C). The lower temperature led to a higher surface area and larger number of active sites for photocatalytic processes (Herrmann, 1999). Another reason is the difference in the energy structure between anatase and rutile as shown in Figure 2.2. In both types, the position of the valence band is similar, which are very low, meaning that, the resulting positive holes show sufficient oxidative power. On the other hand, the conduction band that positioned near the oxidation-reduction potential of the hydrogen shows that anatase is higher in the energy diagram, meaning that, the reducing power of the anatase type is stronger than rutile type. This is very important to drive the reaction for the reduction of molecular oxygen to O<sub>2</sub><sup>•-</sup> radical anion, which is as important as the •OH radicals in degrading the organic pollutants (Sumita *et al.*, 2002; Carp *et al.*, 2004). Due to the difference in the position of conduction band and formation temperature, the anatase type exhibits higher overall photocatalytic activity than the rutile type.

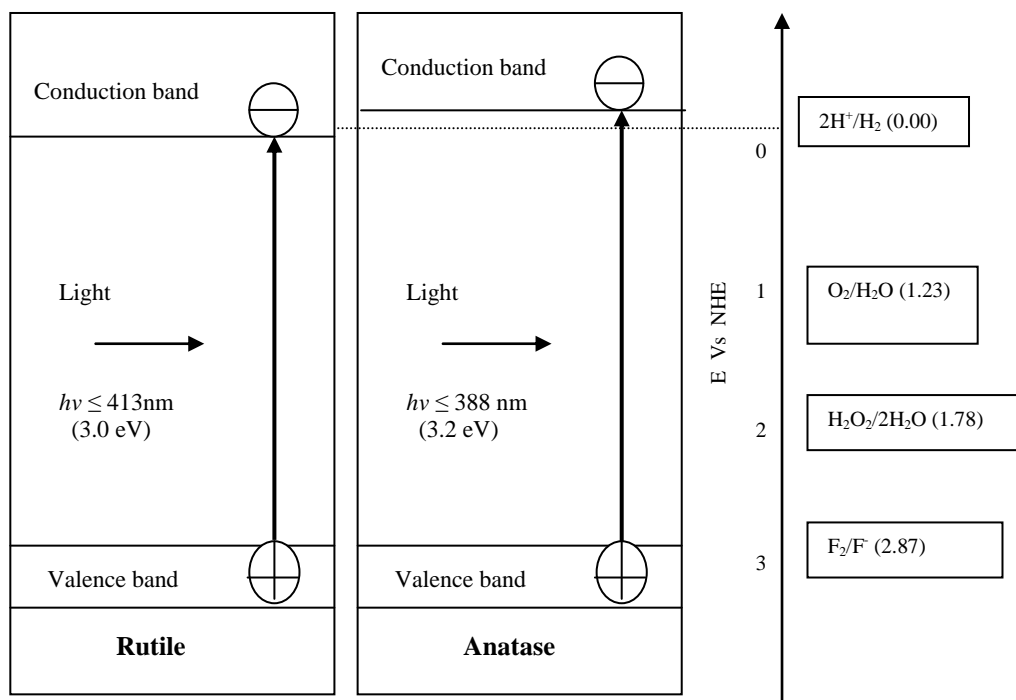


Figure 2.2: Energy diagram for TiO<sub>2</sub> and relevant redox potentials (Mills and Hunte, 1997).

### 2.2.2 Titanium dioxide assisted photocatalysis

During the photocatalytic process, TiO<sub>2</sub> is activated under an irradiation of UV light and established a redox reaction in the aqueous solution. TiO<sub>2</sub> absorbs impinging photons with energies equal to or higher than its band gap, resulting an electron in the occupied valence band of the TiO<sub>2</sub> elevated to the unoccupied conduction band, leading to generation of conduction band electron ( $e_{cb}^-$ ) and valence band hole ( $h_{vb}^+$ ) (Alhakimi *et al.*, 2003; Fernandez *et al.*, 2004). The electron-hole generation in TiO<sub>2</sub> is very fast, usually in femtoseconds, is illustrated in Figure 2.3.

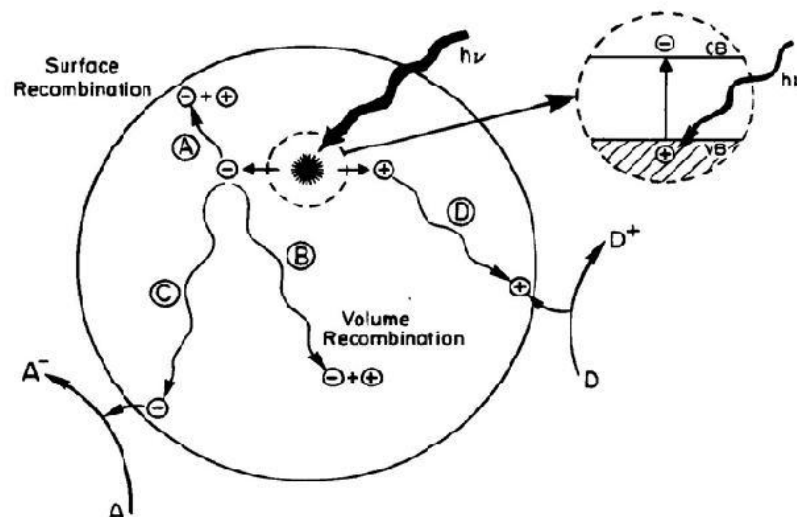
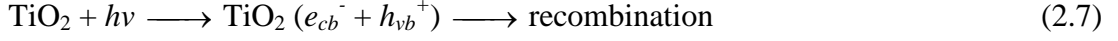


Figure 2.3: Schematic representation of the processes occurring in photocatalysis upon irradiation of  $\text{TiO}_2$  (Koči *et al.*, 2008).

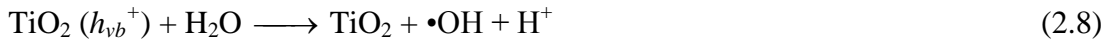
Subsequently, the separated electron and hole could follow several possible pathways. Migration of electrons and holes to the  $\text{TiO}_2$  surface is followed by transfer of photogenerated electrons to adsorbed molecules or solvents. The electron transfer process is more efficient if the species are pre-adsorbed on the  $\text{TiO}_2$  surface. While at the surface of  $\text{TiO}_2$ , electrons are donated to reduce an electron acceptor (pathway C). On the other hand, holes can migrate to the surface, where they can combine with electron from donor species to oxidize the donor species (pathway D) (Tariq *et al.*, 2005; Koči *et al.*, 2008). In competition with charge transfer to adsorbed species is electron and hole recombination. Recombination can occur in the volume and at the surface of  $\text{TiO}_2$  (pathway B and pathway A) (Koči *et al.*, 2008).

Once the charge separation is maintained (pathways C and D), both charge carriers are migrated to the  $\text{TiO}_2$  surface. Therefore, a series of reaction is generated in the  $\text{TiO}_2$  assisted photocatalysis activity (Equations 2.7 to 2.16). Equation 2.7 represents the formation of the charge carriers upon the illumination of the  $\text{TiO}_2$ . If

the generated charge carriers are not involved in any further reactions, they can quickly recombine (Robertson *et al.*, 2005).



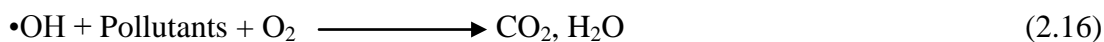
Consequently, the photogenerated holes can react with water or OH<sup>-</sup> group and oxidize them into •OH radicals. Relevant reactions for the hole trapping is expressed in Equation 2.8 and Equation 2.9 (Pirkanniemi and Sillanpää 2002; Konstantinou and Albanis, 2004).



On the other hand, the photogenerated electrons can react with electron acceptor such as O<sub>2</sub> to form superoxide ions (Equation 2.10). Subsequently, a series of further reaction could occur to form •OH radicals (Equations 2.11 to Equation 2.15) (Litter, 1999; Pirkanniemi and Sillanpää 2002).



The resulting •OH radicals are very strong oxidizing agent which can oxidize the organic pollutants into less harmful compounds such as CO<sub>2</sub> and H<sub>2</sub>O as expressed in Equation 2.16 (Gaya and Abdullah, 2008).



### 2.3 NANOSIZED TITANIUM DIOXIDE

Since the photocatalytic processes is affected by adsorption of the substrate onto the surface of TiO<sub>2</sub>, the size of the photocatalyst is important in photocatalytic process. Recent studies suggested that many of the issues involving wastewater treatment could be greatly improved using nanostructure catalyst (Jang *et al.*, 2001; Liu *et al.*, 2005; Wu *et al.*, 2005). In their review, Thiruvengkatachari *et al.* (2008) mentioned that the effect of particle size on the photocatalytic activity can be interpreted in term of surface area. Generally, the smaller the particle size of TiO<sub>2</sub>, the larger the available surface area of TiO<sub>2</sub> and the higher the TiO<sub>2</sub> photocatalytic activity. They reported that the major advantage of nanosized TiO<sub>2</sub> was to provide a larger number of active sites located at the surface, leading to greater adsorbability of the pollutants on the TiO<sub>2</sub> surface.

Jang *et al.* (2001) had showed that greater photocatalytic activity can be achieved by nanosized TiO<sub>2</sub>. In their study, they found that the photocatalytic degradation of methylene blue increased as the diameter of TiO<sub>2</sub> decreased from 30 nm to 15 nm. They explained that the surface area of TiO<sub>2</sub> highly correlated to the particle size. Higher photocatalytic activity can be obtained with higher surface area



for larger contact area between the photocatalyst and target material. While larger surface area can be obtained by decreasing the particle size of the photocatalyst.

Wu *et al.* (2005) studied the photocatalytic degradation of Mordant Yellow (MY) using mesoporous nanocrystalline TiO<sub>2</sub>. Their results revealed that the photocatalytic activity of TiO<sub>2</sub> was related to their surface area and particle size. They noted that smaller particle size not only provided larger surface area but also shorten the route on which an electron from the conduction band of the photocatalyst migrated to its surface. Their works also explained that high surface area of TiO<sub>2</sub> can provide more active sites and adsorb more pollutant molecules.

Liu *et al.* (2005) investigated the photocatalytic degradation of Rhodamine B using Zn<sup>2+</sup>-doped TiO<sub>2</sub> nanoparticle (Zn/TiO<sub>2</sub>). They stated in their work that the particle size of TiO<sub>2</sub> was important to enhance the photocatalytic efficiency. Their results showed that Zn/TiO<sub>2</sub> with smaller particle size, about 10 nm, enhanced the photocatalytic activity greatly, compared to TiO<sub>2</sub> that has crystal size about 20-30 nm. They attributed this result by the fact that the smaller particle size would lead to the photocatalyst having larger surface area, which increase the adsorption of reactant and light, and thus improve the photocatalytic activity.

However, fine TiO<sub>2</sub> in nanometer sized limit its practical applications because of the additional separation processes required to recover the ultrafine catalyst at the end of the treatment. Therefore, attempts have been made to synthesize the immobilized nanosized catalyst on a diverse selection of supports.

## 2.4 SYNTHESIS OF IMMOBILIZED PHOTOCATALYST

The physical and chemical properties of immobilized TiO<sub>2</sub> especially its particle size are strongly related to the preparation methods. Basically, there are two types of preparation methods for preparing the immobilized TiO<sub>2</sub>:

### 1) Gas-phase methods:

- Chemical vapour deposition (CVD) (Gianluca *et al.*, 2008)
- Spray pyrolysis deposition (SPD) (Carp *et al.*, 2004)

### 2) Liquid-phase methods:

- Sol-gel method (Chin *et al.*, 2004)
- Hydrothermal method (Kang, 2002)

Both methods are competitive in producing the immobilized TiO<sub>2</sub>. However, liquid-phase method usually found more convenient and appealing. Sol-gel and hydrothermal methods have been reported to be the most common liquid-phase method to produce the immobilized TiO<sub>2</sub> (Kang, 2002; Chin *et al.*, 2004; Choi *et al.*, 2006). Kang (2002) prepared TiO<sub>2</sub> immobilized on pyrex plate using sol-gel and hydrothermal methods. In their study, they found that both films prepared from sol-gel and hydrothermal methods were stably attached on the supports, except that some cracks were formed on the film attained from the sol-gel method. Furthermore, by analyzing the particle size distribution in colloidal solution attained from both methods, they discovered that TiO<sub>2</sub> particle prepared by hydrothermal method was ranged from 25 nm to 45 nm, whereas the sol-gel method gave a larger TiO<sub>2</sub> particle that ranged from 30 nm to 100 nm. Both immobilized TiO<sub>2</sub> were then tested in a

batch reactor for the degradation of paraquat. The results showed that the activity of immobilized TiO<sub>2</sub> prepared by hydrothermal method gave much higher degradation efficiency than the sol-gel method. They reported that immobilized TiO<sub>2</sub> prepared by the hydrothermal method gave 100 % of degradation at an irradiation time of 15 hours, while for immobilized TiO<sub>2</sub> prepared by the sol-gel method; only 90 % degradation of paraquat can be achieved at an irradiation time of 25 hours. Their work explained that the TiO<sub>2</sub> samples derived by sol-gel method were amorphous in nature, requiring further heat treatment at a high temperature to induce crystallization. The high temperature can give rise to small surface area, crystal growth and undesirable phase transformation from anatase to rutile, and consequently decreased the efficiency of photocatalytic degradation.

Yu *et al.* (2005) prepared TiO<sub>2</sub> nanocrystal using sol-gel and hydrothermal methods. They found that photocatalyst prepared by the sol-gel method gave a larger particle size compared to those prepared by the hydrothermal method. TiO<sub>2</sub> with larger particle size of 40 nm was obtained via calcination (sol-gel), whereas the TiO<sub>2</sub> with 5 nm particle size was obtained by hydrothermal treatment. Thus, development of process without the calcination step for crystallization may be more favourable.

## **2.5 HYDROTHERMAL METHOD**

Hydrothermal is a method that has been widely applied in industrial processes for preparing ceramic samples (Byrappa and Adschiri, 2007). Recently, hydrothermal method is also known as one of the excellent processes that can be employed as an alternative to calcination for the preparation of TiO<sub>2</sub> in a nanocrystalline state (Kang, 2002; Kolen'ko *et al.*, 2003; Yu *et al.*, 2005). Using hydrothermal method to

synthesize TiO<sub>2</sub> is advantageous, as no special equipment other than an autoclave is needed. Additionally, this method is environmental friendly because the reactions are carried out in a closed system (Yu *et al.*, 2005). The physiochemical properties of the prepared TiO<sub>2</sub> can be determined by controlling sol preparation parameters such as concentration and nature of precursor, hydrothermal temperature, experimental duration, pressure and pH of the solutions (Kim *et al.*, 2006). However, in this study, all the parameters were kept constant except the hydrothermal temperature.

Lu and Wen (2008) studied the effect of pH on the photocatalyst preparation in the pH range of 4.0 to 7.0. In their study, they found that the particle size of TiO<sub>2</sub> significantly depended on the pH value of the solution. Their results showed that the particle size of TiO<sub>2</sub> increased as the pH value of the solution increased. They explained that the pH of the solution determined the concentration of OH<sup>-</sup> groups in the solution. As the pH increased, the concentration of OH<sup>-</sup> groups joined with the Ti<sup>4+</sup> complex center also increased. Through the dehydroxylation in the hydrothermal treatment, linkage between Ti-OH increased leading to an increase in the particle size of TiO<sub>2</sub>.

Yu *et al.* (2007b) prepared mesoporous TiO<sub>2</sub> at different hydrothermal temperature and duration. Their results showed that physiochemical properties of TiO<sub>2</sub> significantly influenced by hydrothermal temperature and duration. They noted that with increasing hydrothermal temperature or duration, the crystallinity and particle size of TiO<sub>2</sub> increased. In contrast, the surface area of TiO<sub>2</sub> steadily decreased. Furthermore, by analyzing the photocatalytic activity of prepared photocatalyst, they discovered that increasing hydrothermal temperature or duration

increased the degradation efficiency. The best hydrothermal condition (180°C for 10 hours) was determined on the acetone degradation. They explained that the desirable crystallinity, particle size and surface area of the prepared photocatalyst, leading to the best enhancement during the degradation of acetone.

Wang *et al.* (2009b) studied the effect of hydrothermal temperature on TiO<sub>2</sub> preparation. In their study, they found that increasing the hydrothermal temperature increased the particle size and crystallinity, and thereby decreased the surface area of TiO<sub>2</sub>. Their results also showed that the degradation efficiency increased when the hydrothermal temperature increased. Maximum degradation efficiency was achieved at hydrothermal temperature of 180°C. They concluded that adequate crystallinity, particle size and surface area were responsible for the observed result.

## **2.6 SUPPORTS FOR IMMOBILIZATION**

Various supports have already been proposed as catalyst support for the photocatalytic degradation of organic pollutants. These supports included glass (Fernández *et al.*, 1995), quartz (Fernández *et al.*, 1995; Lu *et al.*, 1999), stainless steel (Fernández *et al.*, 1995; Shang *et al.*, 2003; Zhao *et al.*, 2007), cotton (Tryba, 2008), perlite (Na *et al.*, 2005; Hosseini *et al.*, 2007); zeolite (Ökte and Yilmaz, 2008; Mahalakshmi *et al.*, 2009); silica gel (Zhang *et al.*, 2006) and activated carbon (Liu *et al.*, 2007; Ao *et al.*, 2008; Sun *et al.*, 2009).

Studies with TiO<sub>2</sub> immobilized on several rigid supports were carried out by Fernández *et al.* (1995) on photocatalytic degradation of malic acid. The supports that used in their study were glass, quartz and stainless steel. They reported that the